Supplementary Information for A robust high-content imaging approach for probing the mechanism of action and phenotypic outcomes of cell cycle modulators

Supplementary Methods

Cell culture and compound treatment

HCT-116 cells were grown according to ATCC guidelines. Adherent cells were plated onto poly-D-lysine coated 96-well dishes (BD #356640) at a density of 3,000 cells per well in 100 µl of media as determined by a Coulter Z2 cell and particle counter. Cells were incubated with compounds in a final concentration of 0.5% DMSO. All compounds were prepared as ten-point concentration curves using two-fold dilutions and a starting concentration of 5 µM for experiment 1, and 2 µM for experiments 2 and 3. Compound dilutions and additions were performed using a Multimek-96 automated pipettor (Beckmann). The first column contains DMSO only (negative control), and the last contains nocodazole at a concentration of 0.2 µM (positive control).

Immunofluorescence

Cells were fixed with 3.7% formaldehyde for 20 minutes at 37°C and permeabilized with 0.1% Triton-X 100 for 10 minutes at 25°C. All subsequent dilutions were performed in PBS at 25°C. Fixative was removed and each well washed with PBS. Cells were blocked using 1% Bovine Serum Albumin (BSA) (Invitrogen #15260-037) for 1 hour at 25°C. The primary antibodies against phosphorylated-histone H3 (Upstate Biolabs #06-570) and cyclin B1 (BD Pharmingen #624086) were diluted in 1% BSA to a final concentration of 5 µg/ml and this mixture added to each well for 1 hour at 25°C. Each well was then washed 3 times with 200 µL of PBS, and incubated for 1 hour at 25°C with a solution containing 5 µg/ml goat α-mouse-Alexa-488 (Molecular Probes #A-11029) to detect cyclin B1,

5 μg/mL goat α-rabbit-Alexa-647 (Molecular Probes #A-21244) to detect pHH3, and 200 ng/ml Hoechst 33342 to detect nuclear material (Molecular Probes #21492). For experiment 1, TUNEL analysis was then performed using the Roche *in situ* cell death detection kit with TMR-red (Roche # 12 156 792 910) and stored at 4°C until analysis. For experiment 3, the primary antibody against α-tubulin (Sigma #T6074) was diluted in 1% BSA to a final concentration of 1 μg/ml, treated as above, and detected with 5 μg/ml goat α-mouse-Alexa-555 (Molecular Probes #A-21422).

Fluorescent imaging and image analysis

Cell images were captured using a Cellomics Arrayscan VTI and analyzed with the Target Activation bio-application V.3 reading in 4 channels at a magnification of 10X. Objects were identified using an algorithm to detect nuclear staining with Hoechst dye, and the relative levels and sub-cellular localization of cyclin B1 and pHH3 were determined through the respective intensities and locations of Alexa-488, and Alexa-647 fluorescence. The relative levels and sub-cellular localization of both TUNEL and α-tubulin were determined in their separate experiments by the intensity and localization of Alexa-555 fluorescence. A minimum of 1000 individual cellular images or 20 fields were captured for each condition. Nuclear and cytoplasmic features were defined from cellular objects, and used for quantifying cellular phenotypes. For features related to cyclin B1 and α-tubulin, a cytoplasmic mask is defined by extending 10 pixels beyond the nuclear mask.

Enzyme assays

Kinase cell-free assay data displayed on the kinome in Figure 5 and Supplementary Figure 8 were obtained from in-house assays, the Millipore Kinase Profiler service

(http://www.millipore.com/drugdiscovery/dd2/kinasetarget, accessed May 4, 2010) and the CEREP kinase profiling service (http://www.CEREP.fr/CEREP/Users/pages/ProductsServices/kinasePlatform.asp; accessed May 4, 2010). All assays use activated kinases. The majority of results are obtained from the CEREP service, using thru-plate screening at 0.2, 2 and 20 μM followed by fitting of 3 point IC_{50} values with the bottom and top asymptotes constrained to 0% and 100%, respectively, and the Hill coefficient to 1. Extrapolation is limited to 3 fold from the lowest / highest concentrations; values of <0.067 μM appearing on the figures arise from curves where the extrapolated IC_{50} occurs at concentrations below 0.067 μM. Determination of 3 point IC_{50} values in a manner similar to what has been described elsewhere[1] is cost-effective and generally yields results comparable to 10 point IC_{50}s from internal assays, often in different assay formats from those used at CEREP/Millipore: 70% of results are within 3 fold of the 10 point IC_{50}, 80% within 5 fold, 90% within 10 fold.

All results with $IC_{50} \leq$ 10uM for CDK1, CDK4, CDK7, CDK9, AURKA, AURKB and PLK1 come from the same internal assay; inactive results (i.e. % inhibition < 80 at 20 μM or IC_{50} >10 μM) from CEREP/Millipore profiling were usually not repeated internally (e.g. not retesting in internal CDK assays a PLK inhibitor found to be inactive in CEREP/Millipore CDK assays).

Kinase	**Technique**	**Substrate**
CDK1	Filter binding	Histone H1 peptide
CDK4	Filter binding	C-terminal retinoblastoma fragment
CDK7	Transcreener	CDK7/9 peptide
CDK9	Transcreener	CDK7/9 peptide
AURKA	Filter binding	AURKA activation loop peptide
AURKB	Filter binding	Histone H3 peptide
PLK1	Filter binding	GSTcdc25c(1-206)

1. Turner, R. J.; Charlton, S. J. Assessing the minimum number of data points required for accurate IC50 determination. *Assay Drug Dev Technol* **2005,** 3, 525-31.

Supplementary Scheme 1

Aurora Inhibitors

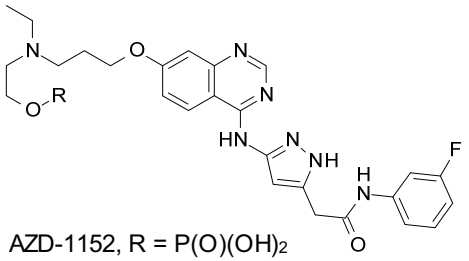

AZD-1152, R = $P(O)(OH)_2$
AZD-1152 metabolite, R = H

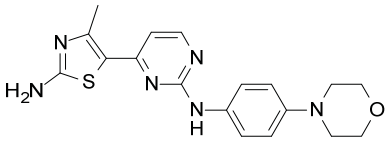

CYC116

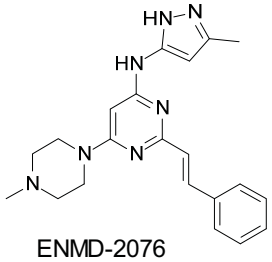

ENMD-2076

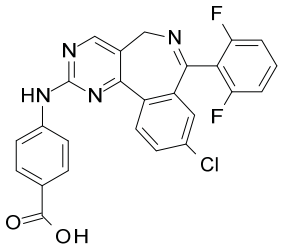

MLN-8054

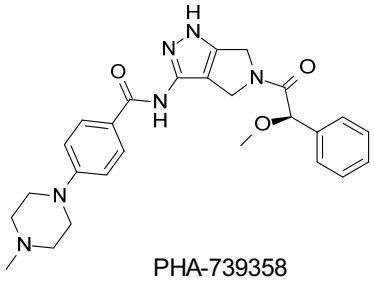

PHA-739358

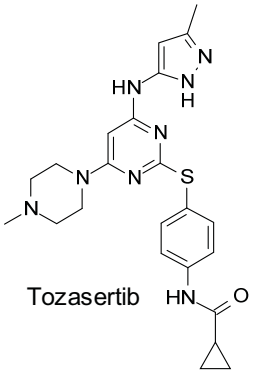

Tozasertib

CDK Inhibitors

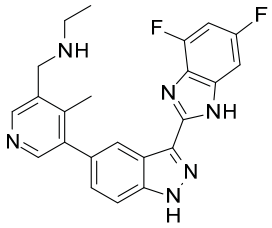

AG-024322

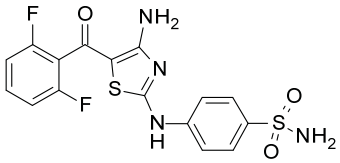

AG-12286

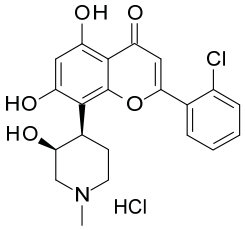

Alvocidib

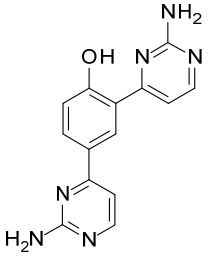

BMI-1026

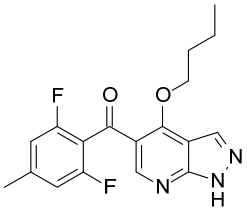

BMS-265246

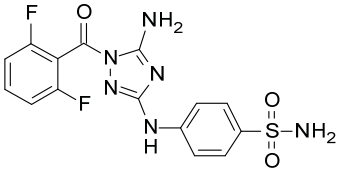

JNJ-7706621

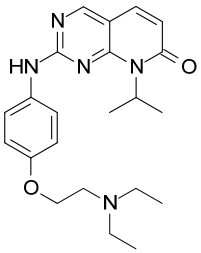

PD-171851

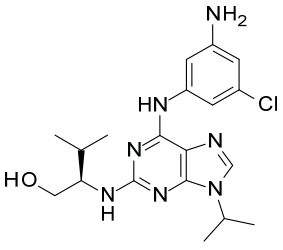

Aminopurvalanol

Supplementary Scheme 1 (continued)

CDK Inhibitors (continued)

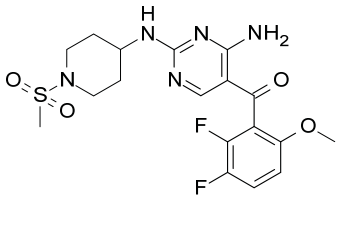

R-547

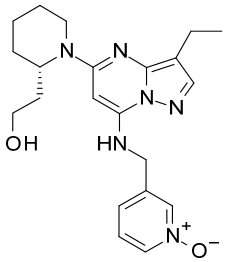

SCH-727965

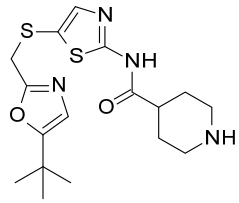

SNS-032

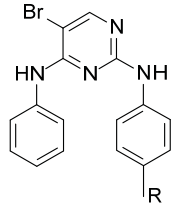

358789-50-1
R=O(CH$_2$)$_2$NEt$_2$
358788-29-1
R=C(O)NH(CH$_2$)$_3$N(nBu)$_2$

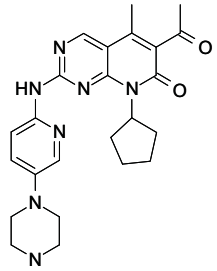

PD-332991

PLK1 Inhibitors

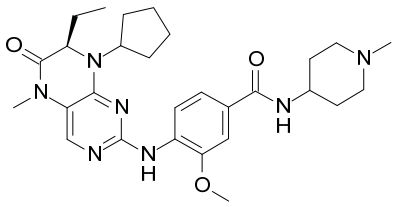

BI-2536

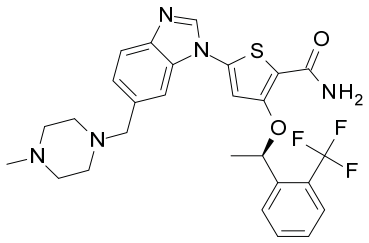

GSK-461364

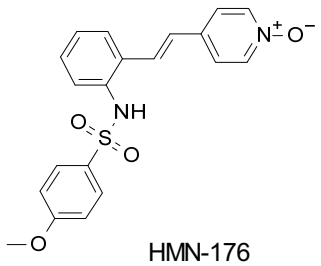

HMN-176

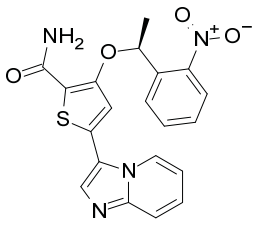

886856-66-2

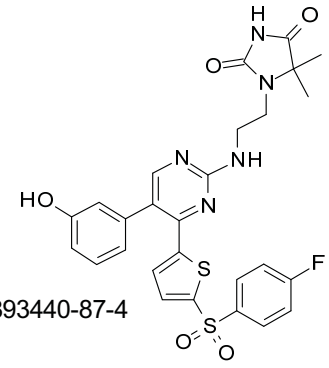

893440-87-4

Supplementary Scheme 1 (continued)

Wee1 Inhibitor

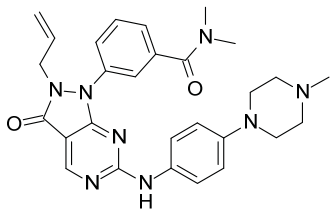

955365-24-9

DNA Intercalators/Topoisomerase Inhibitors

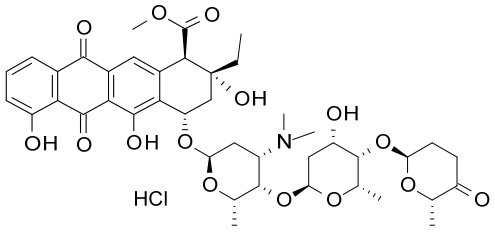

Aclarubicin

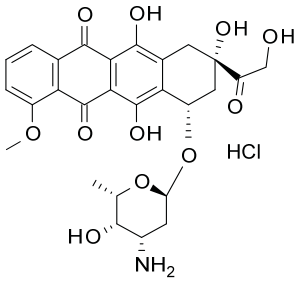

Doxorubicin

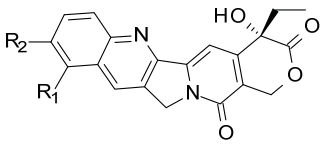

Camptothecin
$R_1=R_2=H$
Topotecan
$R_1=CH_2NMe_2$, $R_2=OH$

DNA Synthesis Inhibitors

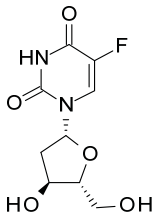

5-Fluoro-2'-deoxyuridine

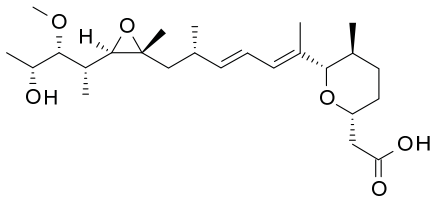

Herboxidiene

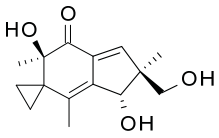

Illudin S

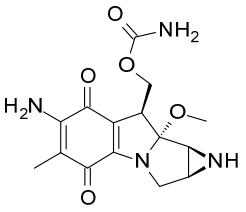

Mitomycin

Microtubule Modulators

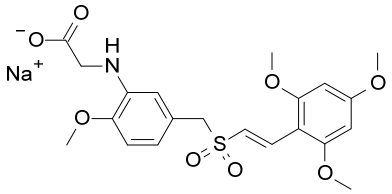

ON-01910.Na

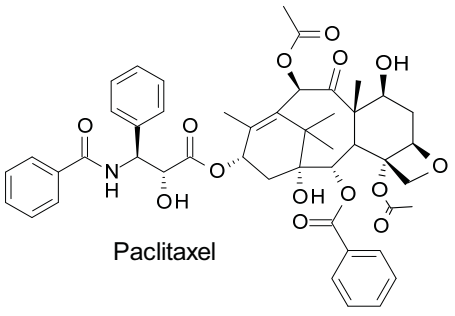

Paclitaxel

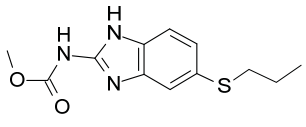

Albendazole

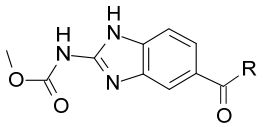

Ciclobendazole, R = Cyclopropyl
Mebendazole, R = Phenyl
Nocodazole, R = 2-Thiophenyl

Supplementary Table 1. Cytological features employed for quantifying cell phenotypes

Feature	Description	Significance
ObjectTotalIntenDNA	Total DNA intensity	DNA content: 2N, S-phase, 4N, 8N, etc.
ObjectAvgIntenDNA	Average DNA intensity	cells in mitosis have high DNA intensity
ObjectVarIntenDNA	Variation in DNA intensity	Measures variation in DNA intensity across pixels, correlated with ObjectAvgIntenDNA
ObjectAreaDNA	Nuclear Area	Increases as cell progresses from G_1, S, G_2, then decreases sharply at the G_2/M boundary
ObjectShapeLWRDNA	Nuclear length-width ratio	High LWR with high ObjectAvgIntenDNA indicates formation of metaphase plate
ObjectShapeP2ADNA	Nuclear perimeter vs. area ratio	High P2A often indicates polyploidy, due to multi-lobed nature of nuclei clusters
TotalIntenCycB	Total Cyclin B1 intensity	Activates CDK1, increased from S through G2/M, dissipates in metaphase
AvgIntenCycB	Average Cyclin B1 intensity	TotalIntenCycB divided by area of cytoplasmic mask
VarIntenCycB	Variation in Cyclin B1 intensity	Variation in pixel intensity within cytoplasmic mask
TotalIntenPH3	Total phospho-histone H3 intensity	Elevated in prophase to metaphase, dissipates in anaphase
AvgIntenPH3	Average PH3 intensity	TotalIntenPH3 divided by area of nuclear mask
VarIntenPH3	Variation in PH3 intensity	Variation in pixel intensity within nuclear mask
TotalIntenTUNEL	Total TUNEL intensity	A measure for apoptosis through the use of DNA end labeling
AvgIntenTUNEL	Average TUNEL intensity	TotalIntenTUNEL divided by area of nuclear mask
VarIntenTUNEL	Variation in TUNEL intensity	Variation in pixel intensity within nuclear mask
TotalIntenTub	Total α-tubulin intensity	Examined for its potential in differentiating microtubule modulators
AvgIntenTub	Average α-tubulin intensity	TotalIntenTub divided by area of cytoplasmic mask
VarIntenTub	Variation in α-tubulin intensity	Variation in pixel intensity within cytoplasmic mask

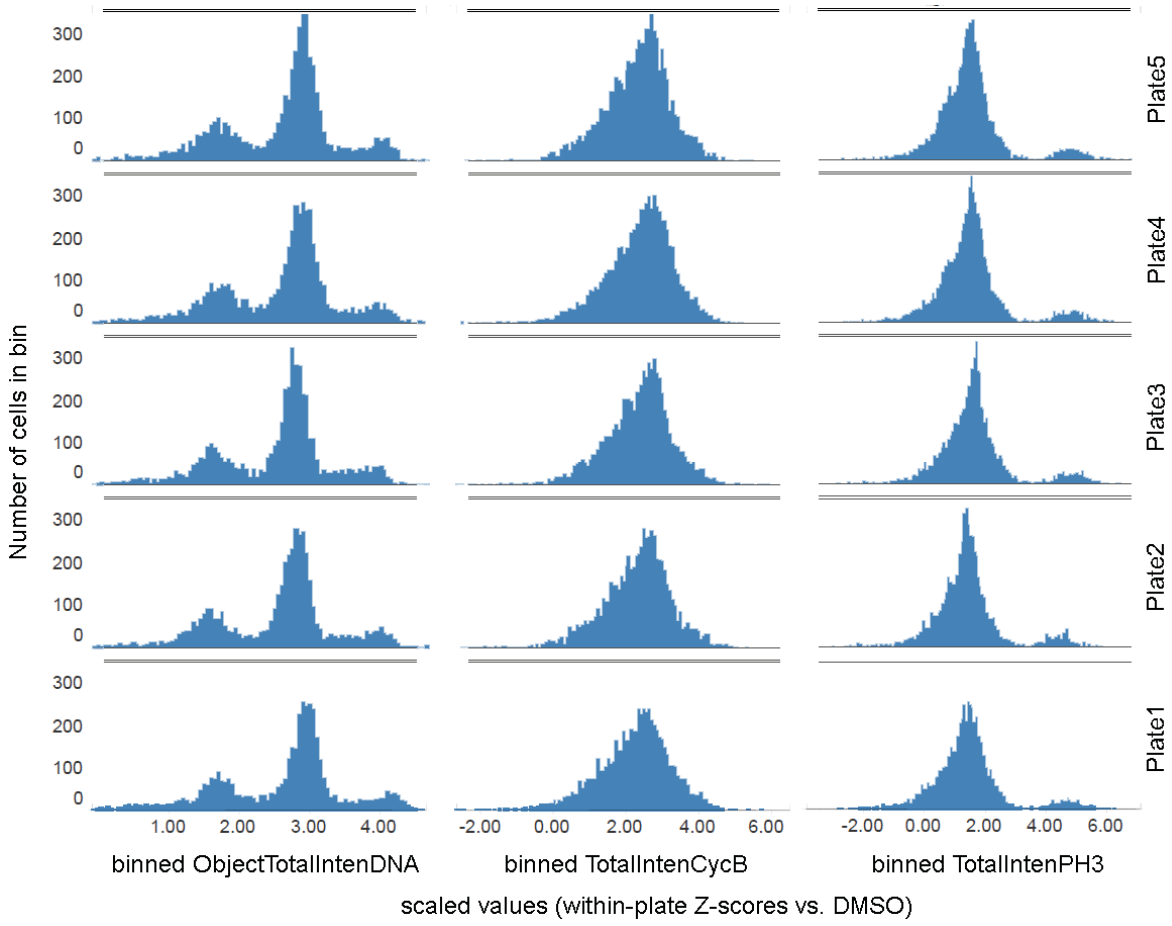

Supplementary Fig. 1 Histograms showing distributions of intensity in cell populations treated with 0.2 μM of nocodazole, obtained by pooling 8 positive control wells per 96-well plate. Each row shows the distribution of intensities within a single plate. Column 1 corresponds to DNA (Hoechst staining), column 2 is Cyclin B1 and column 3 is phospho-histone H3. Numerical values on the X-axis (ranges binned into 200 equal intervals) are Z-scores measuring the distance in standard deviations from DMSO-treated cells (Methods). This visualization is used to verify plate-to-plate reproducibility within a single experiment.

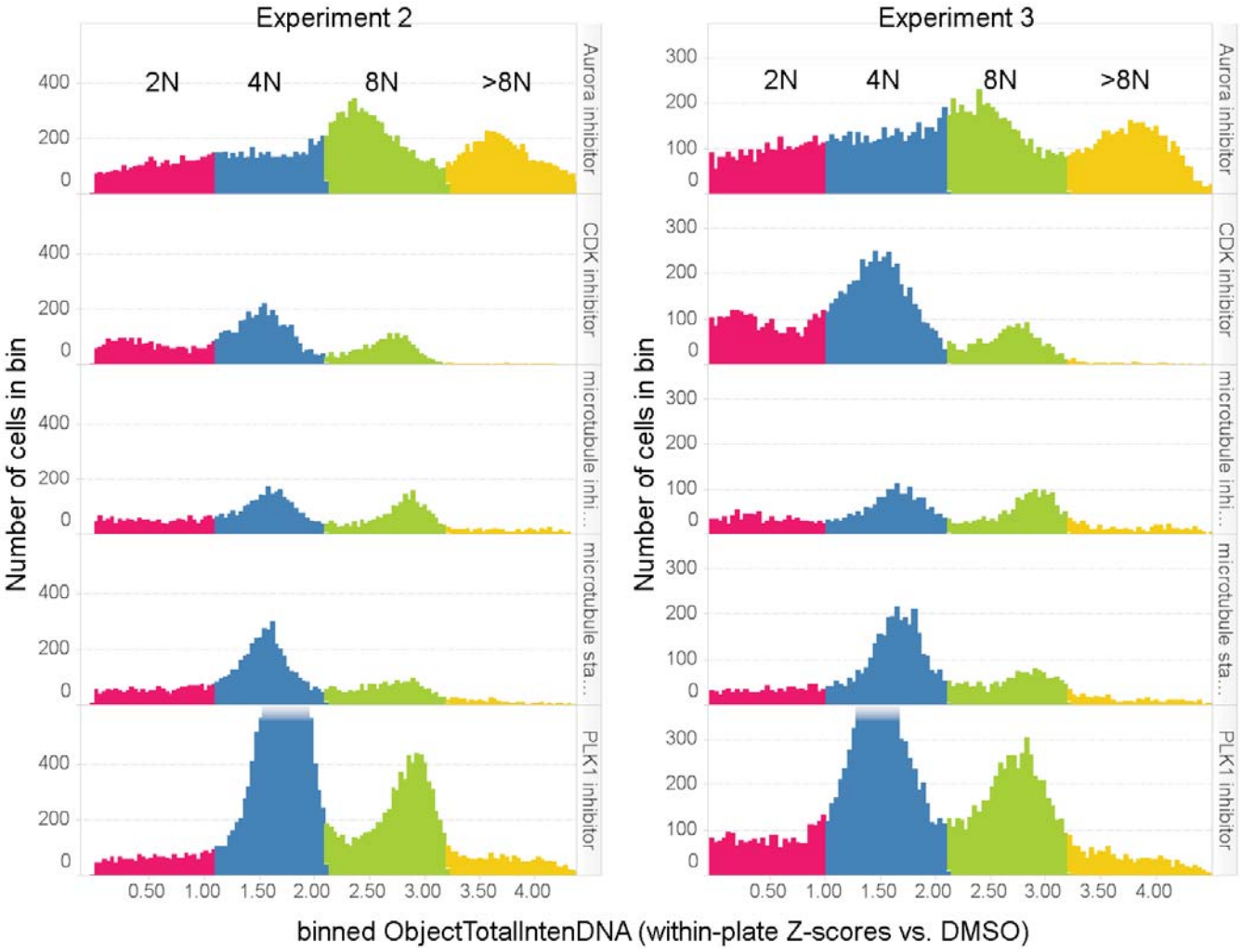

Supplementary Fig. 2. Histograms showing distribution of total DNA intensity obtained by pooling cells treated with 8 calibration compounds (Table 1); only wells with concentrations above the anti-proliferation EC_{50} are used. Numerical values on the X-axis (ranges binned into 200 equal intervals) are Z-scores measuring the distance in standard deviations from DMSO-treated cells (Methods). The distribution is binned manually into ranges corresponding to 2N (pink), 4N (blue), 8N (green) and >8N (yellow) DNA content, with the objective of establishing DNA classification rules that separate 2N, 4N, 8N and >8N for the 5 mechanistic classes. The boundaries are not optimal for each mechanistic class in isolation, due to variation in Hoechst staining that arises from variation in DNA coiling. The reference compounds were selected since they induce cell phenotypes consistent with their mechanism of action in all wells above the EC_{50}, allowing those wells to be pooled. The aurora inhibitors yield enriched populations of 8N and >8N cells, with the latter arising from segmentation errors in identifying nuclei; the CDK and PLK 1 inhibitors yield enriched populations of 4N cells, and smaller populations of apparent 8N and >8N cells. See text for interpretation of apparent multinucleation for non-aurora mechanisms.

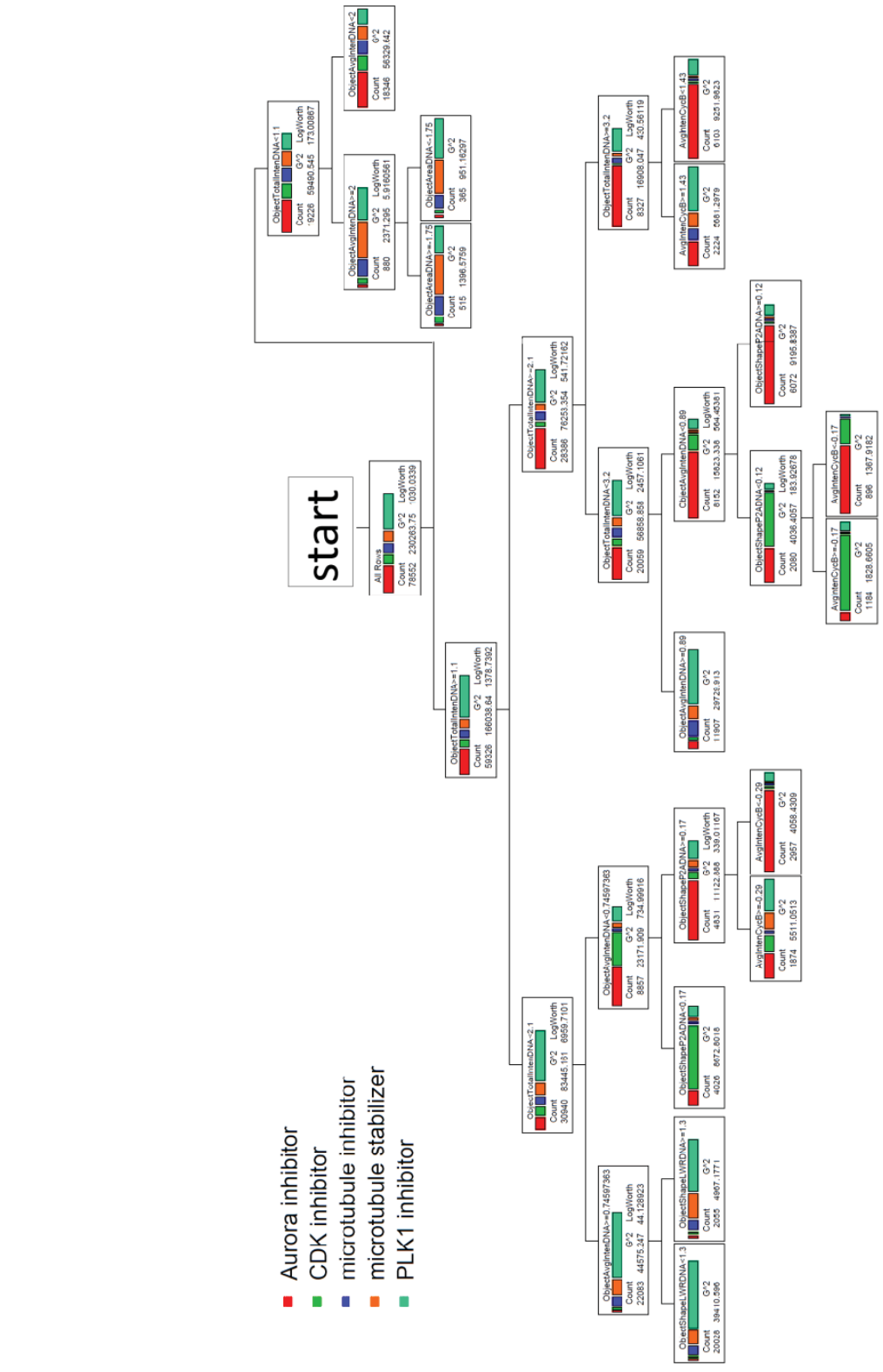

Supplementary Fig. 3. View of the recursive partitioning model in Jmp, as defined from experiment 3; the splits using ObjectTotalIntenDNA are defined by selecting the feature and split value manually. See Methods for details.

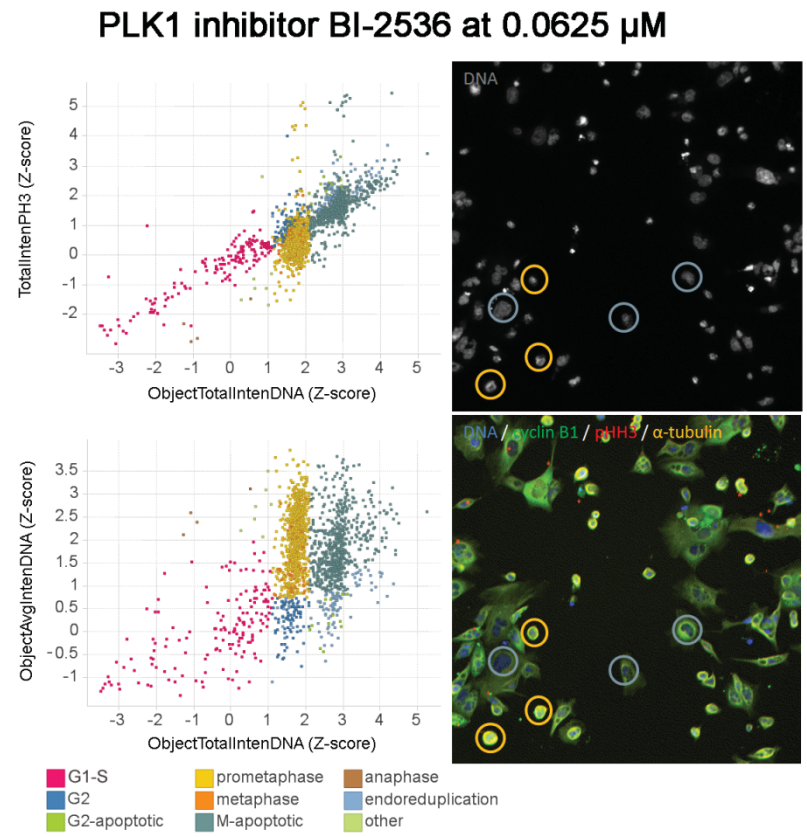

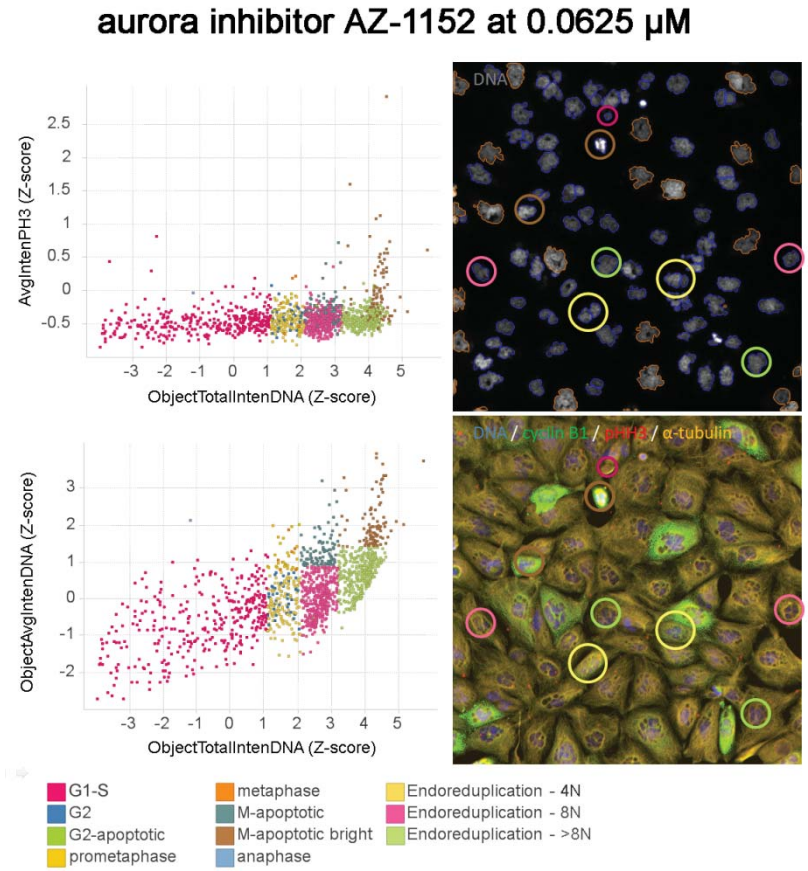

Supplementary Fig. 4 (continued)

Supplementary Fig. 4 Scatter plots showing selected cytological features, with cells colored according to phenotype from the cell classifier (left panels), and fields of view for DNA alone or all 4 channels combined (right panels; DNA=blue; CyclinB1=green, pHH3 = red, α-tubulin = yellow). Representative cells are identified using circles colored as indicated in the scatter plot; the PLK1 inhibitor BI-2536 at 0.0625 µM (top) and the aurora inhibitor AZ-1152 at 0.0625 µM (bottom). For AZ-1152, the DNA channel image shows nuclei segmentation boundaries, with rejected objects shown in brown. Objects exceeding the maximum size threshold of 1200 pixels^2 were rejected.

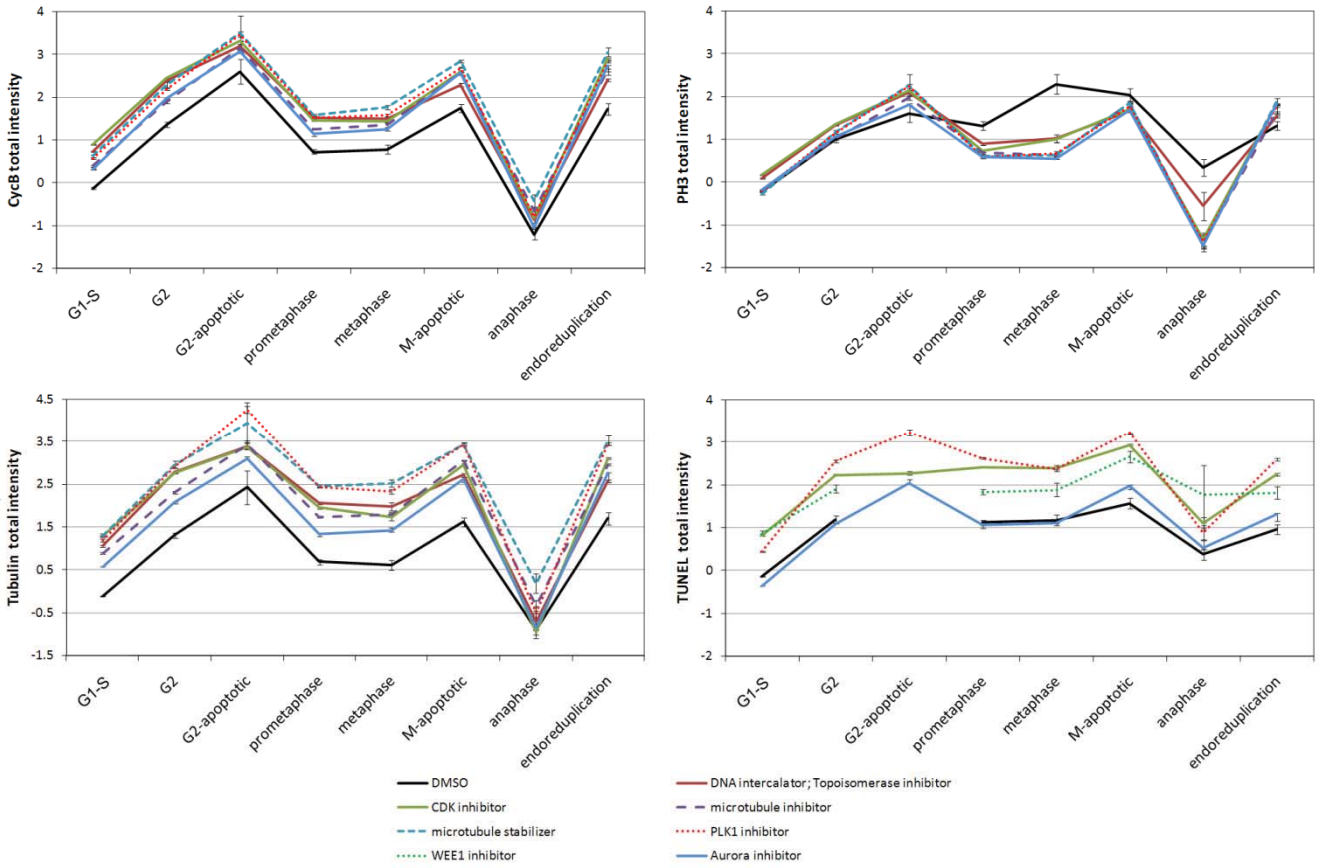

Supplementary Fig. 5 Line charts showing normalized total cyclinB1, pHH3, α-tubulin from experiment 3, and TUNEL intensity values from experiment 1, for cells belonging to each phenotype class. Each series denotes the average and standard error of the mean for cells treated with compounds of a given mechanism; only wells having concentration above the EC_{50} are used. The large error bars for G2-apoptotic cells occurring from DMSO and microtubule stabilizer treatments, and anaphase cells from Wee1 treatment arise due to the occurrence of <15 cells of those types.

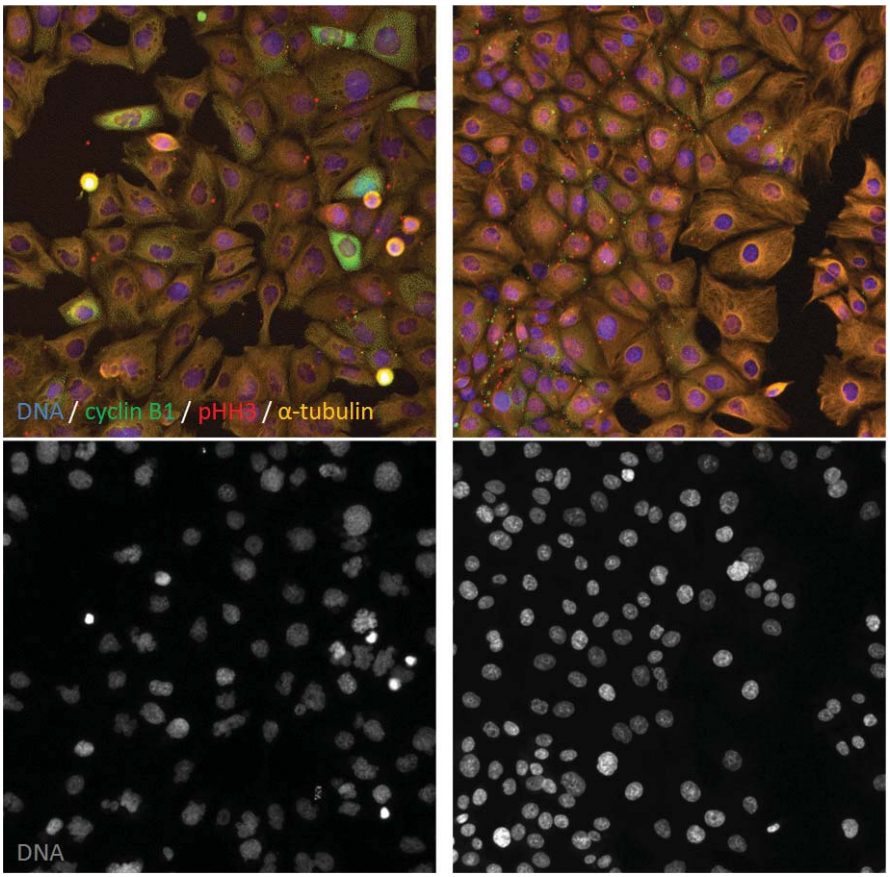

Supplementary Fig. 6 Contrasting the comparison of treatments using well averages vs. cell population profiles for the aurora inhibitor tozasertib at 0.25 μM (left) with the CDK inhibor R-547 at 0.5 μM. Tozasertib induces a mixed cell population of multinucleated cells with large diffuse nuclei, and M-phase apoptotic cells with smaller bright nuclei. An "average" cell (which does not exist in the population) has values of cytological features similar to those observed in the more uniform population of G_2 arrested cells responding to treatment with R-547.

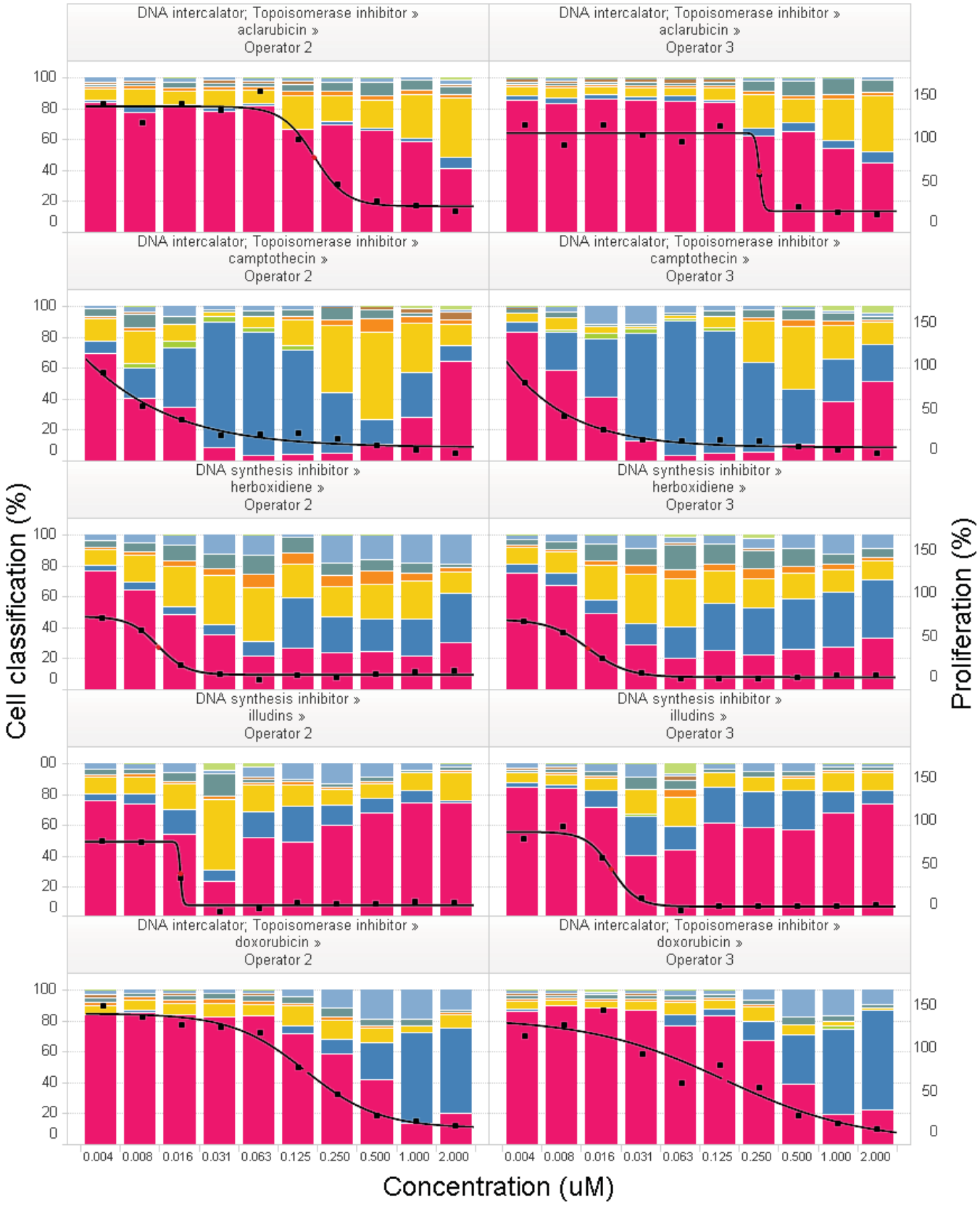

Supplementary Fig. 7 (continued)

Supplementary Fig. 7 (continued)

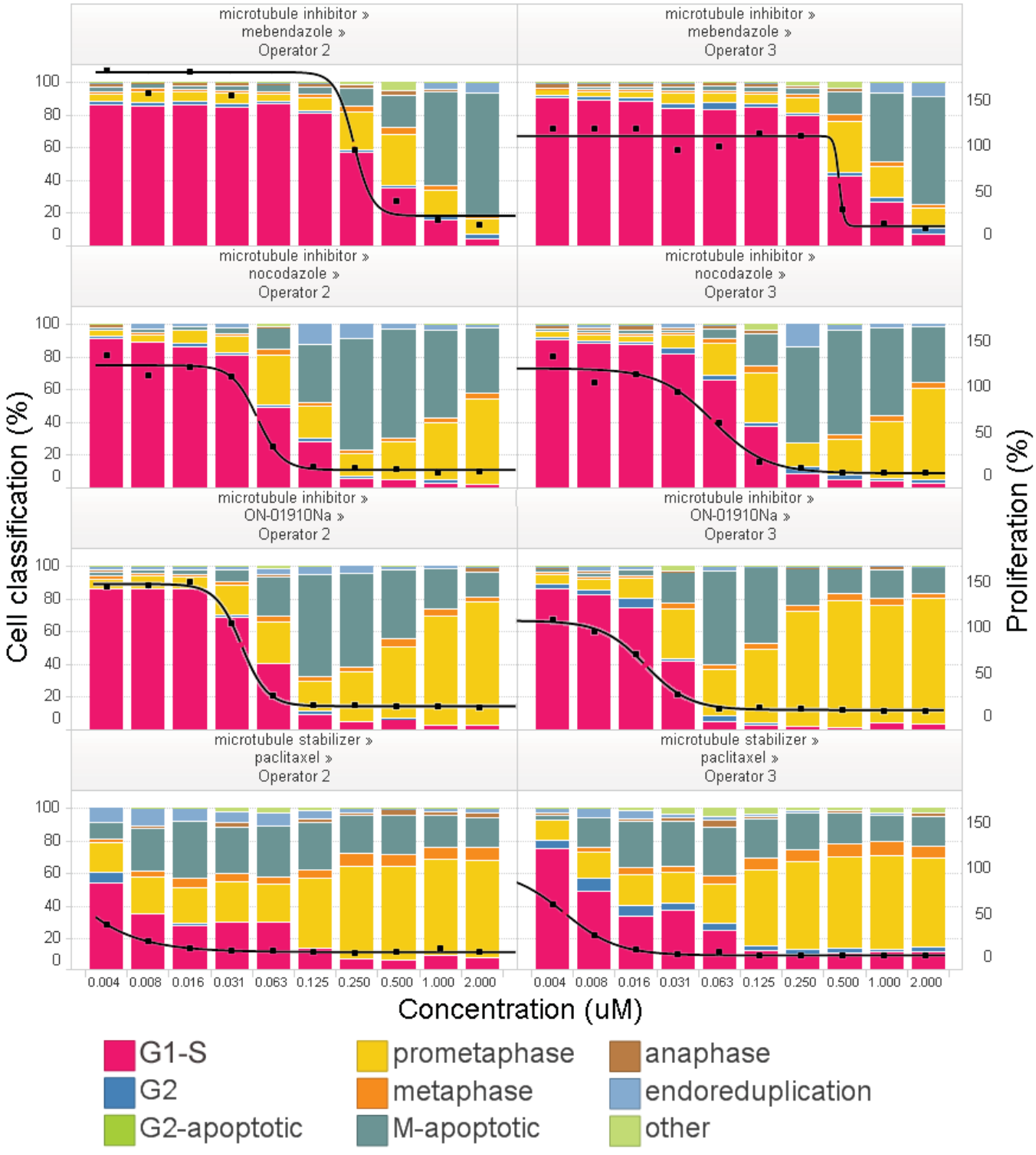

Supplementary Fig. 7. Proportion of HCT-116 cells classified into each of 9 phenotypes vs. concentration for non-kinase cell cycle modulators characterized in experiments 2 (left panels) and 3 (right panels). The curve indicates inhibition of proliferation measured by counting cells per field of view.

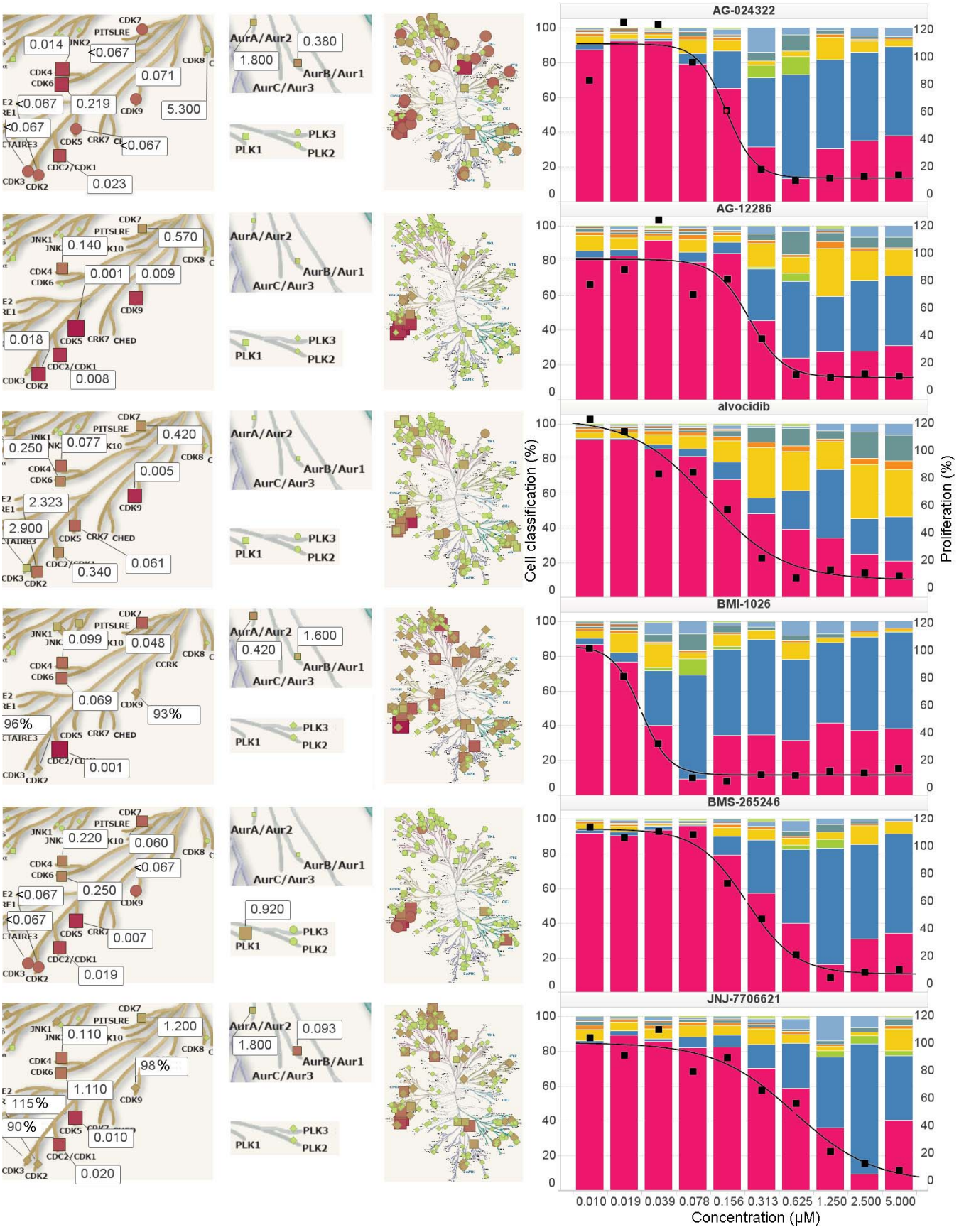

Supplementary Fig. 8 (CDK inhibitors; continued)

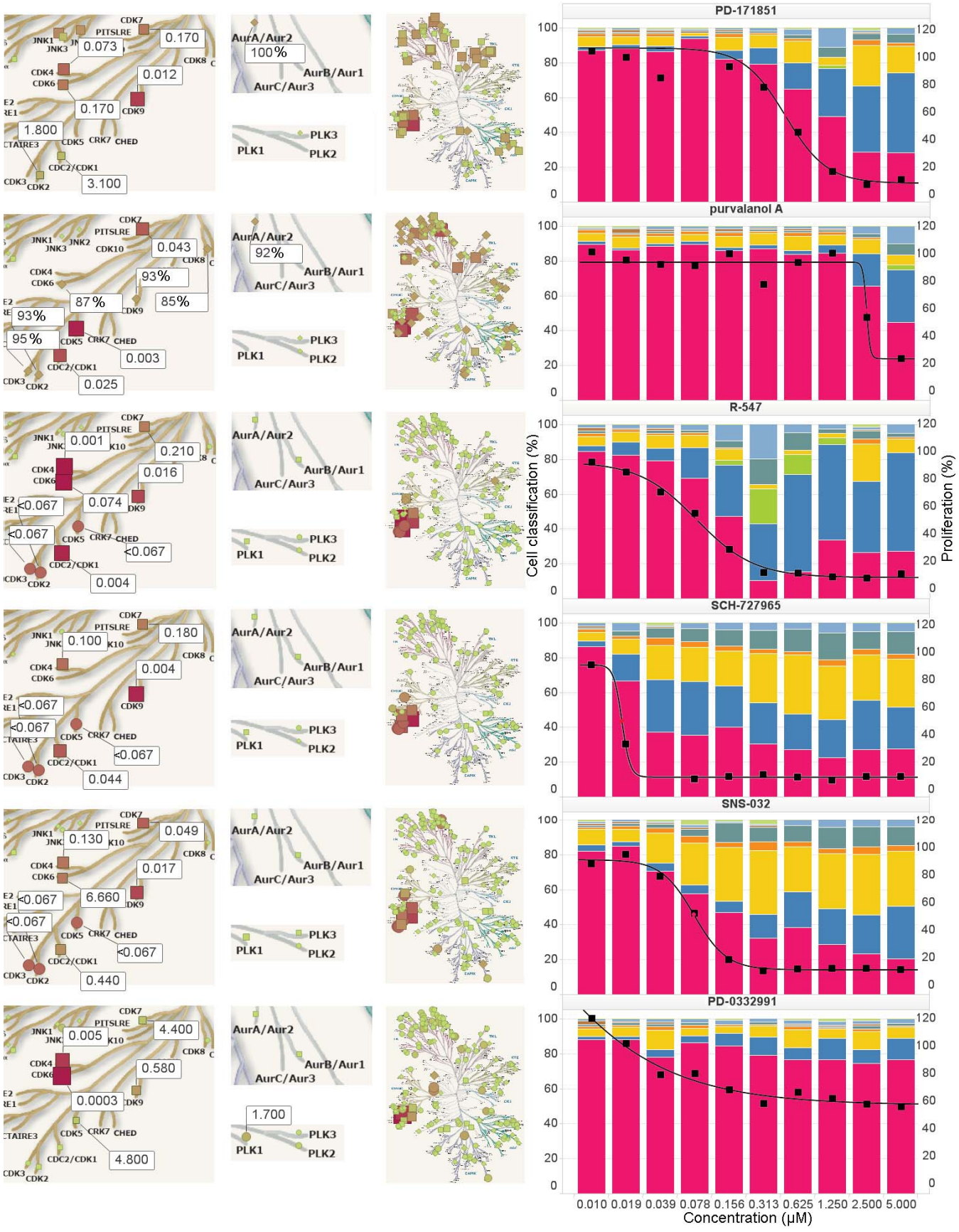

Supplementary Fig. 8 (CDK inhibitors; continued)

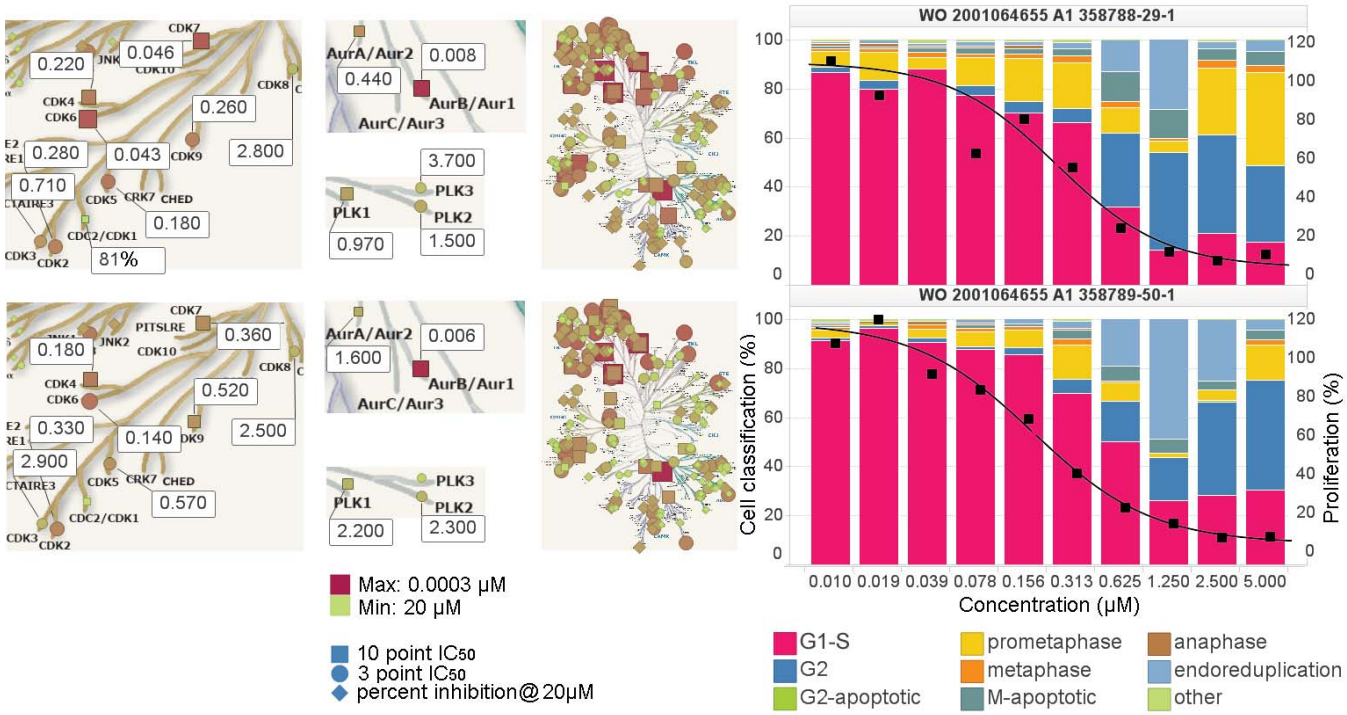

Supplementary Fig. 8 (CDK inhibitors, continued)

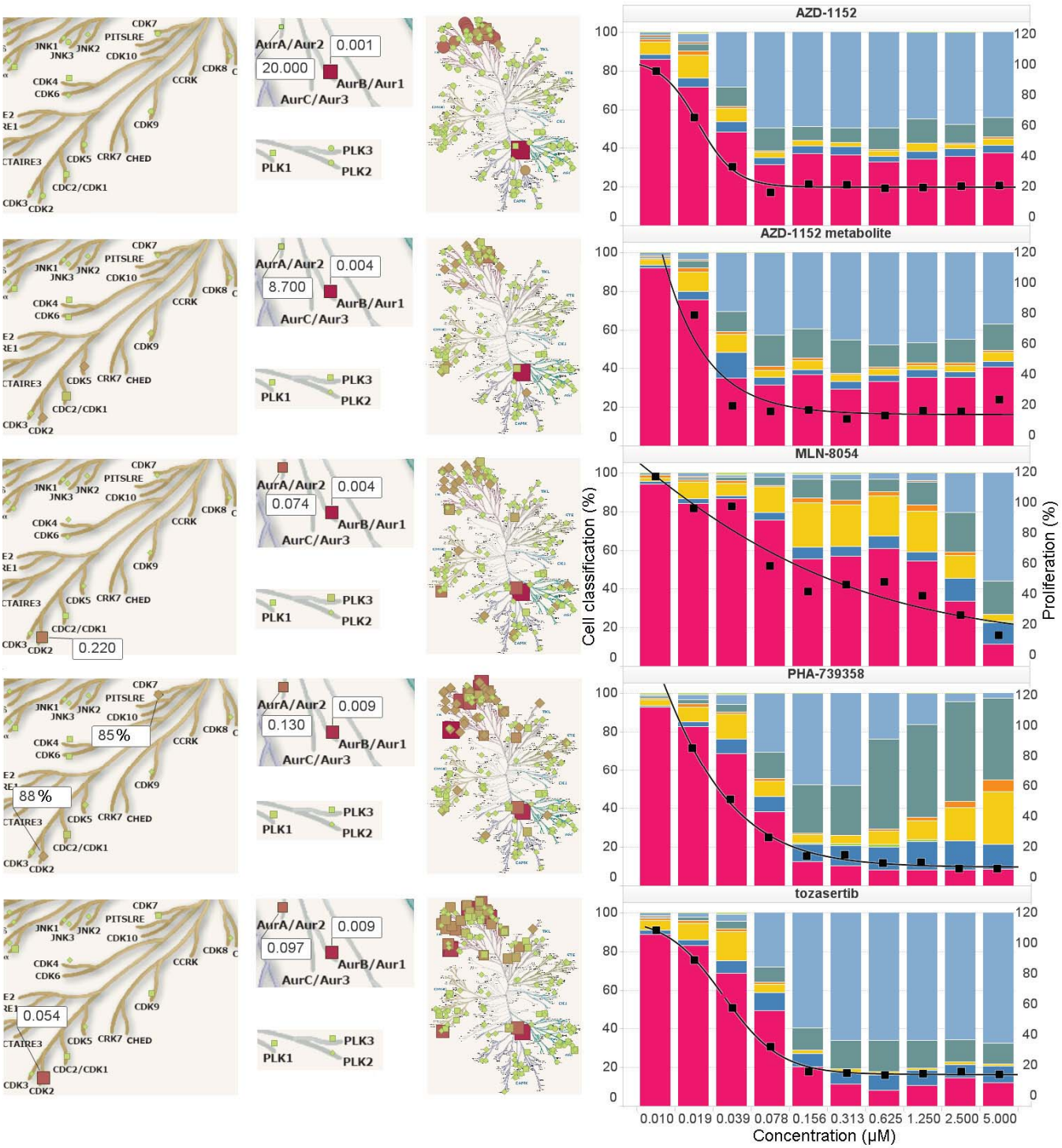

Supplementary Fig. 8 (aurora inhibitors, continued)

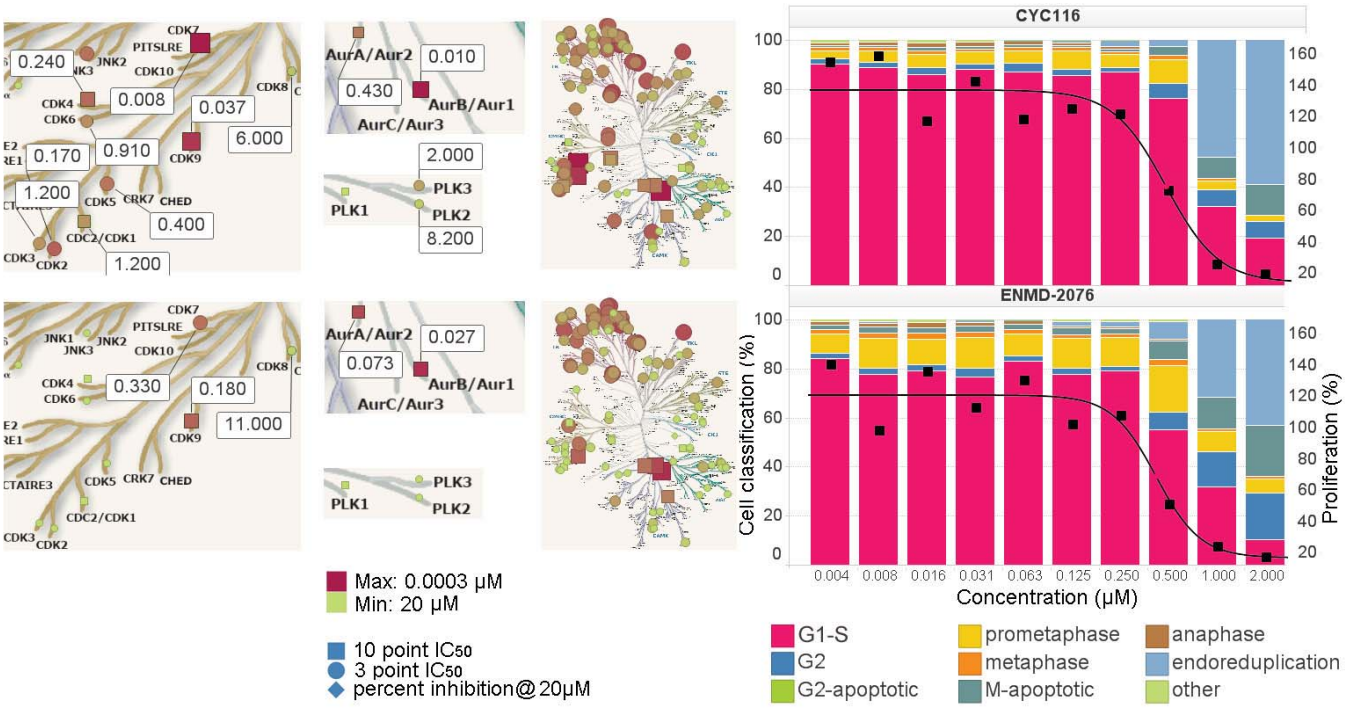

Supplementary Fig. 8 (aurora inhibitors, continued)

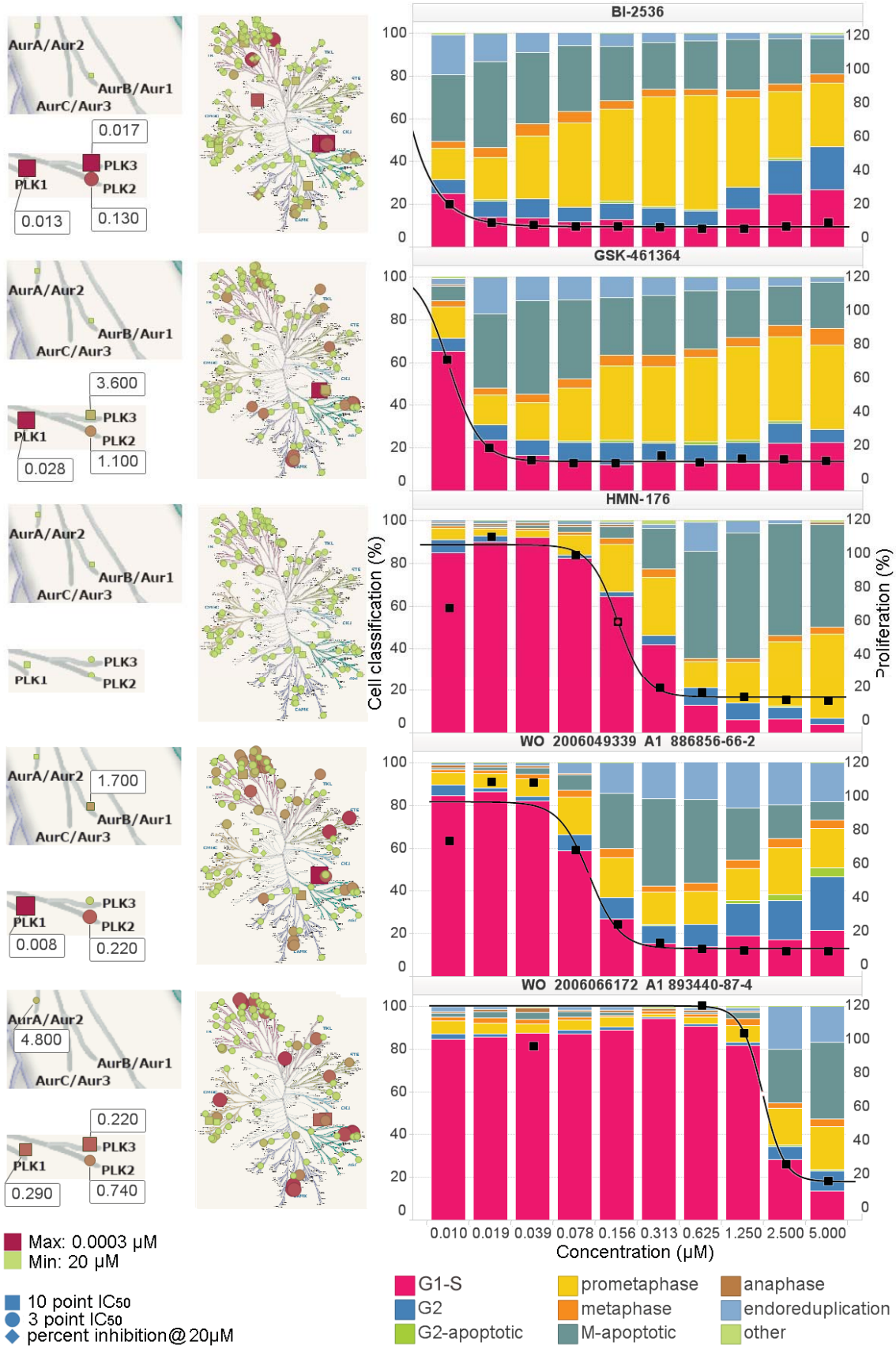

Supplementary Fig. 8 (PLK1 inhibitors, continued)

Supplementary Fig. 8 Kinase profiling data from biochemical enzyme assays and cell phenotypes in HCT-116 cells. Right panel: proportion of cells classified into each of 9 phenotypes vs. treatment concentration; the curve indicates inhibition of proliferation measured by counting cells per field of view. Left and center panels: results from kinase enzyme assay profiling, with insets showing detail for CDK, aurora and PLK kinases. Changes in markers from green to red (and small to large) indicate increasing binding affinity, on a $\log_{10}$ scale. Labeled markers indicate the IC_{50} in μM (no units) or % inhibition at 20 μM (values followed by %); the absence of labels denote inactive results (i.e. IC50 > 10 μM or % inhibition < 80 for single point results). See Supplementary Methods for details on enzyme assays. Human kinome provided courtesy of Cell Signaling Technology, Inc. www.cellsignal.com.

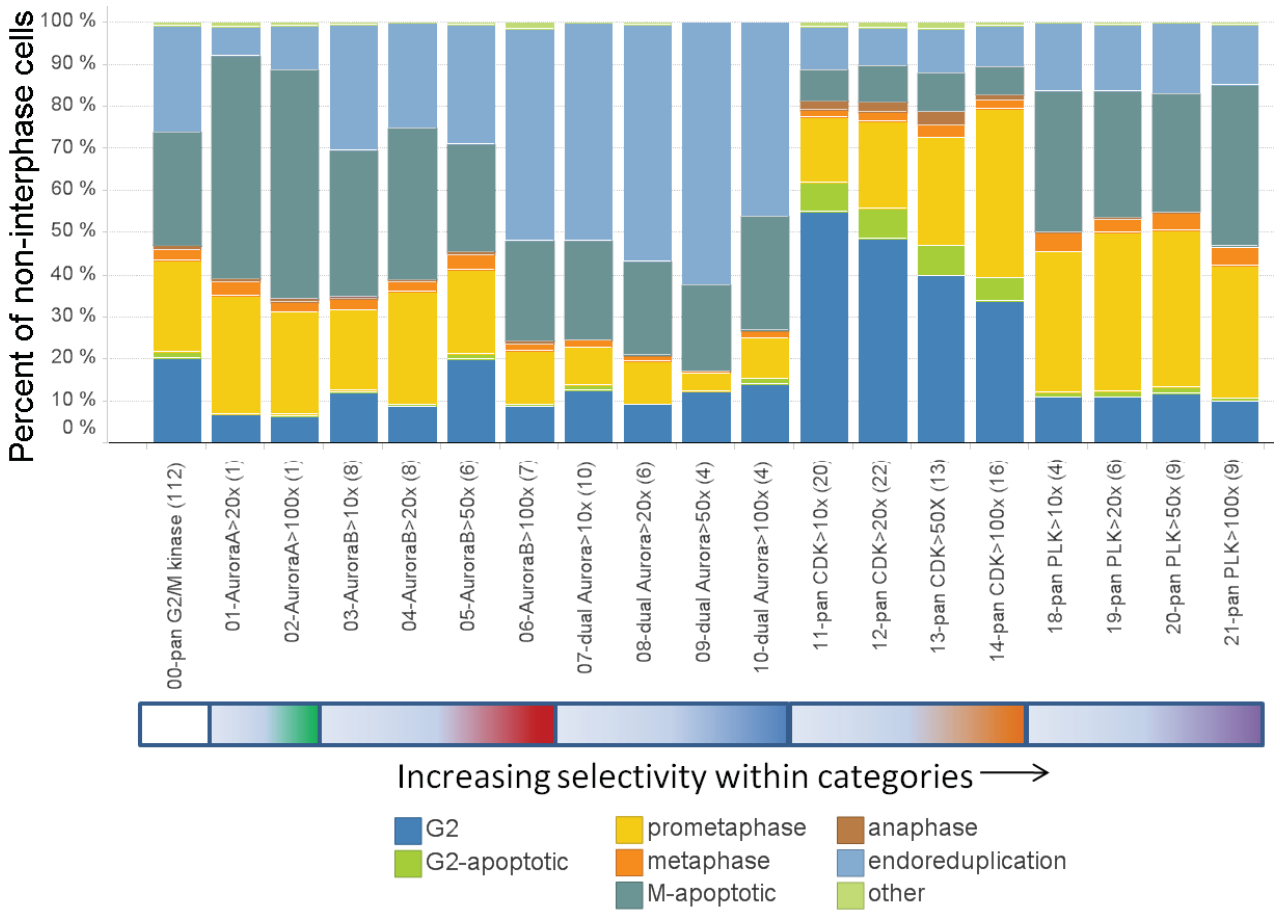

Supplementary Fig. 9 The dependence of cell phenotype on selectivity in enzyme assays, determined using 266 cell cycle inhibitors synthesized for lead optimization programs. All compounds have measured enzyme activity vs. CDK1, AURKA, AURKB and PLK1 and anti-proliferation EC_{50} < 1 μM in HCT-116 cells. For each compound, its selectivity towards the most potently inhibited kinase is expressed as the ratio $IC_{50,\text{ other G2/M kinases}}$ / $IC_{50,\text{ most potent G2/M kinase}}$; large fold differences indicate greater selectivity. The category pan-G_2/M kinase denotes inhibitors having similar affinity for ≥2 out of 4 kinases. For all compounds in a given selectivity category, wells having concentrations above the anti-proliferation EC_{50} in HCT-116 cells were pooled, and the proportion of non- G_1-S cells among all compounds in the selectivity category is calculated by simple average of the proportions for each compound.